# DESIGN, CONSTRUCTION AND FIELD CHARACTERIZATION OF A VARIABLE POLARIZATION UNDULATOR FOR SOLEIL

B. Diviacco, R. Bracco, C. Knapic, D. Millo, D. Zangrando, Sincrotrone Trieste, Italy
O. Chubar, A. Dael, M. Massal, SOLEIL, France
Z. Martí, LLS, Spain

## *Abstract*

Two variable polarization undulators have been designed and are under construction in the framework of a Collaboration agreement between Société Civile Synchrotron SOLEIL and Sincrotrone Trieste. In this paper the main aspects of the magnetic and mechanical design are summarized. Field optimization techniques are described, showing the achieved performance in terms of phase, trajectory and field integral errors.

## MAGNETIC DESIGN

The HU80 undulators, to be installed on the 2.75 GeV SOLEIL storage ring [1], is designed to provide variable polarization in the photon energy range 80 eV to ~2 keV. The APPLE-II structure [2] consists of four permanent magnet arrays. Horizontal, elliptical/circular and vertical polarization is produced when two diagonally opposite arrays (the mobile arrays) are shifted longitudinally in the same direction (parallel mode). On the other hand, skew linear polarization, variable between 0 and 90º, is generated when the two arrays are shifted in opposite directions (anti-parallel mode) [3]. Both operational modes have been implemented in the HU80 undulators.

The magnetic design features 19 full periods of length $\lambda_0$=80.36 mm. Terminations, making use of half size magnetic blocks, have been optimised to provide a small variation of field integrals (~0.4 G·m) over the whole operational range. Transverse block dimensions (28 x 28 mm) have been chosen as a trade-off between magnetic field intensity, homogeneity (field roll-off) and magnetic forces. As can be seen in Table 1, the magnetic arrays are subjected to strong forces (up to 12 kN).

Table 1: Maximum magnetic forces (in kN) acting on the magnet arrays at minimum gap of 15.5 mm in the parallel (P) and anti-parallel (AP) polarization modes.

| | Fixed array | | Mobile array | | Upper/Lower two arrays | |
|---|---|---|---|---|---|---|
| | P | AP | P | AP | P | AP |
| Transverse | 12 | 12 | 12 | 11 | 0 | 4 |
| Longitudinal | 1 | 12 | 1 | 3 | 0 | 13 |
| Vertical | 9 | 9 | 9 | 9 | 18 | 18 |

These forces, that also change sign during array shifting, may cause unwanted distortion of the mechanical support structure, with negative consequence on the undulator field quality. Using larger blocks would only marginally improve the overall field homogeneity, while significantly increasing the magnetic load.

As a magnetic material a high coercivity grade NdFeB (NEOMAX-38VH, transverse die-pressed) was chosen, characterized by $H_{CJ}^{min}$ = 25 kOe and $B_r^{min}$ = 1.22 T. Individual measurement of the magnetization strength and direction was performed by the manufacturer (NEOMAX Co LTD) using a vibrating sample magnetometer. All the blocks were found within the specified ±1% variation in magnetic moment and 1º angular deviation.

Optimum sorting of the blocks within the undulator structure was determined by means of the popular simulated annealing (S.A.) technique [4], using a merit function defined as the weighted sum of trajectory straightness, rms phase error and transverse field integral distributions. Based on previous experience [5], we didn’t expect to obtain quantitative agreement with the predicted distributions, due to the unavoidable inhomogeneity of magnetization affecting the permanent magnet block. However, compared to a random assembly, the initial field quality was found sufficiently good that the foreseen post-assembly correction methods (see below) proved adequate to reach the required magnetic field tolerances.

## MECHANICAL DESIGN AND PERFORMANCE

The mechanical design was developed taking into account both the forces shown in Table 1 and the maximum vertical dimension allowed for the carriage, limited by the height of the ceiling (~2.2 m) in the SOLEIL storage ring. Special attention was given to the anti-parallel mode, that generates a strong longitudinal force on the upper/lower beams. The support was also specified to allow up to 1 mm gap tapering. The design and construction were carried out by RMP S.r.l., Rome, Italy. The size of the stainless steel beams and the dimensions of the supporting brackets were validated by 3D FEM calculations, carried out with a 50% margin with respect to the computed forces of Table 1. The maximum predicted deflection was less than 20 µm.

To test the transverse deformation and validate the design of the phase shifting mechanism (see Figure 1), a 0.8 m stainless steel mobile-fixed beam prototype was developed. To simulate the transverse magnetic forces, a calibrated loaded spring system was constructed, able to generate positive and negative forces distributed along the structure. The measurements showed deformations of less than 20 µm, under the same load conditions as used for the simulation. A similar system was also employed for the acceptance test of the full-size stainless steel beam assembly.

0-7803-8859-3/05/$20.00 ©2005 IEEE

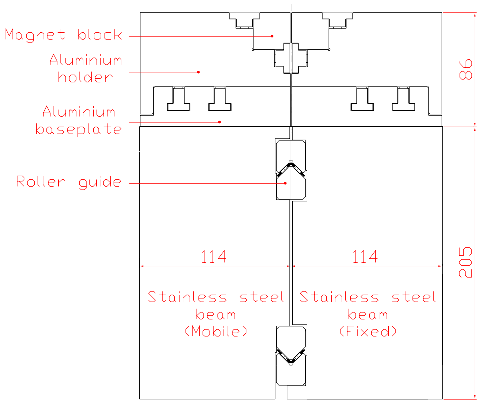

Figure 1: Schematic drawing of the phase shifting mechanism, base-plate and block holders.

Magnet blocks are clamped on individual holders, precisely positioned on a base-plate acting as an interface with the stainless steel beams. By interposition of calibrated brass shims, small horizontal and/or vertical displacement of the blocks are allowed in order to correct for magnetic field imperfections.

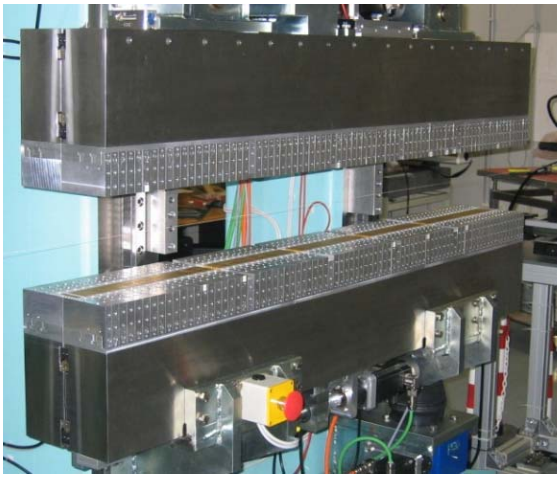

Figure 2: The assembled HU80 undulator

After magnet assembly (see Figure 2), detailed mechanical measurements were carried out with the final magnetic load applied. These measurements, performed at 15 mm gap in parallel/antiparallel mode, showed transverse/longitudinal deformations of the magnetic arrays of less than 50/25 μm.

## CONTROL SYSTEM

A new control system was developed by SOLEIL, within a contract awarded to BERGER LAHR, using the most recent industrial standards. It controls six 3-phase stepping motors (model VRDM 3913) and six absolute linear encoders (TR-Electronic LT) providing 1-2 μm gap and phase accuracy. In addition, each motor has its own rotary encoder for fast motor status control. Safety features include double-contact limit switches and tilt switches mounted on the upper and lower undulator beams. All the equipment is connected to a (PLC-type) TLCC controller via CAN bus. The low-level PLC software was written using the commercial CoDeSys development system. The upper-level control software was written in the CORBA-based TANGO standard.

## MAGNETIC FIELD OPTIMIZATION

After assembly, the undulator field was measured using a Hall-probe bench. The vertical field intensity (0.927 T at the minimum gap of 15.5 mm) closely matches the values predicted by RADIA [6] calculations. Figure 3 shows the trajectories at three representative gaps in the horizontal polarization mode. The corresponding rms optical phase error is 3.0°, 2.7° and 2.4° respectively.

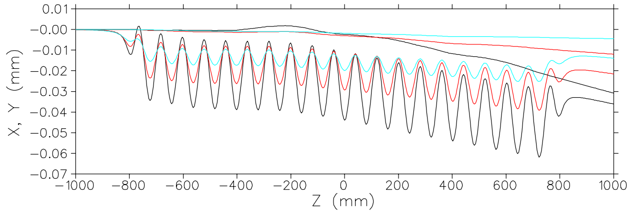

Figure 3: Trajectory computed from measured field for gap of 15.5 mm (black), 30 mm (red) and 50 mm (cyan).

Initial field integrals, measured with a stretched wire system, are shown in Figure 4. No significant dependence of the transverse profiles on the phasing of the arrays has been observed. This indicates that no spurious effect, such as mechanical deformations or interaction of the permanent magnets with ferromagnetic parts, is spoiling the theoretical predictions.

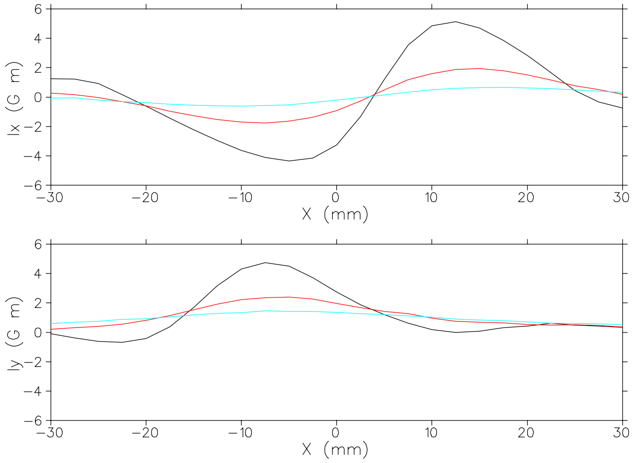

Figure 4: Field integrals measured before shimming at a gap of 15.5 mm (black), 30 mm (red) and 50 mm (cyan).

In order to correct the oscillations of the field integrals and the associated multipole errors, a method using small magnetized cylinders located at the extremities of the device has been developed [7]. An optimum configuration of these magnets, arranged at various horizontal and vertical positions within a specially designed holder (see Figure 5), was found using again a S.A. algorithm. This enabled us to reduce the off-axis field integrals by more than a factor of 3.

Figure 5: Undulator end-section showing the holder for the small correcting permanent magnet pieces.

A further correction was achieved by virtual shimming, a technique consisting in displacing vertically magnetized blocks at selected positions along the undulator. A total of 20 blocks were moved by a maximum of 0.4 mm horizontally and 0.25 mm vertically, thus effectively reducing the vertical aperture from 15.5 to the design value of 15 mm. Once again, a suitable configuration was determined by S.A. based on the computed 'signatures' corresponding to unit horizontal and vertical displacements. As a results, significant improvement in the trajectory straightness, phase error and integrated multipoles was obtained. Figures 6 and 7 show the trajectories and field integrals after correction.

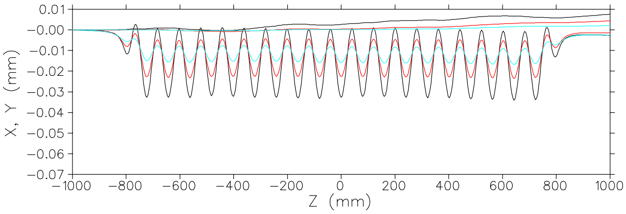

Figure 6: Same as Figure 3 after shimming

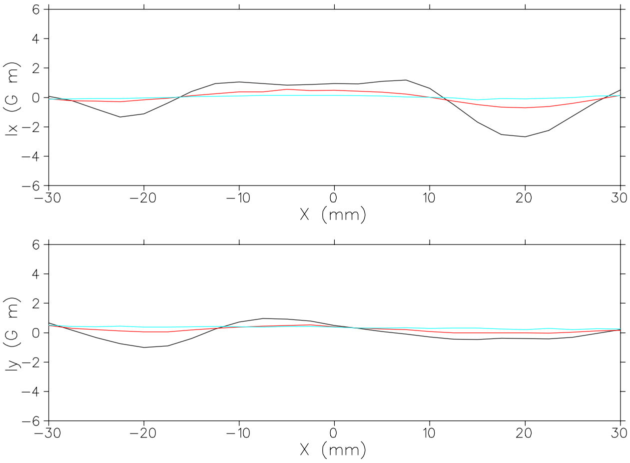

Figure 7: Same as Figure 4 after shimming

Flattening of the field integral profiles was specifically optimized in the range -10 < x < 10 mm. Straightening of the trajectory was achieved together with a reduction of the phase error to less than 1.2º rms at any gap. The field quality was then evaluated in other polarization modes. As an example, Figure 8 shows the trajectory for $Z_S$= 20 mm, corresponding to nearly circular polarization. A maximum phase error of 2.6º was observed in the case of vertical polarization (array shifting $Z_S= \lambda_0/2$).

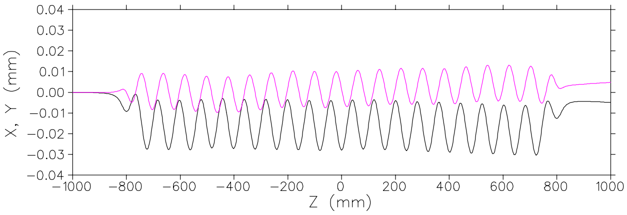

Figure 8: Horizontal (black) and vertical (magenta) trajectory in elliptical polarization mode.

## QUASI-PERIODIC MODIFICATION

Based on specific beamline requirements, the final HU80 undulators will feature a quasi-periodic field in order to reduce the spectral contamination from high-order harmonics. This is achieved by vertical displacement of the horizontally magnetized blocks at a few suitably selected positions along the undulator [8]. At the time of writing, this variant has just been implemented. Figure 9 shows the measured vertical magnetic field for gap=15.5 mm and $Z_S$= 0.

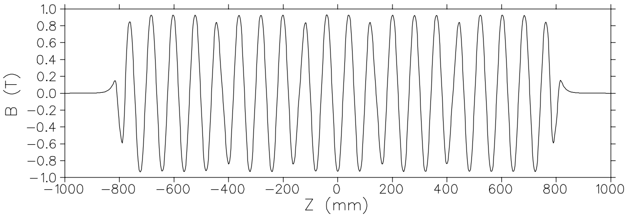

Figure 9: Field of the HU80 quasi-periodic undulator.

The modification is not expected to significantly affect the field integrals. However, should additional correction of the residual errors be necessary, an iteration of the above described shimming process will be applied.

## REFERENCES

[1] O.Chubar et al., Proc. EPAC 2004, p. 369
[2] S.Sasaki, Nucl. Instr. And Meth. In Phys. Res. A 347 (1994) 83.
[3] J.Bahrdt et al., Nucl. Instr. And Meth. In Phys. Res. A 467-468 (2001) 21.
[4] S.Kirkpatrick et al., Science vol. 220, No. 4578 (1983) 671; A.D.Cox, B.P.Youngman, SPIE vol. 582 (1985) 91.
[5] B.Diviacco et al., Proc. EPAC 2000, p. 2322.
[6] O. Chubar et al., J. Synchrotron. Rad. vol.5 (1998), p. 481.
[7] B.Diviacco, Sincrotrone Trieste Technical Note ST/SL-04/01.
[8] B.Diviacco and R.P.Walker, Sincrotrone Trieste Technical Note ST/M-97-11; J.Chavanne, Proc. EPAC 1998, p. 2213.